

# Propensity for *cis*-Proline Formation in Unfolded Proteins

T. Reid Alderson, Jung Ho Lee, Cyril Charlier, Jinfa Ying, and Ad Bax\*<sup>[a]</sup>

In unfolded proteins, peptide bonds involving Pro residues exist in equilibrium between the minor *cis* and major *trans* conformations. Folded proteins predominantly contain *trans*-Pro bonds, and slow *cis*–*trans* Pro isomerization in the unfolded state is often found to be a rate-limiting step in protein folding. Moreover, kinases and phosphatases that act upon Ser/Thr–Pro motifs exhibit preferential recognition of either the *cis*- or *trans*-Pro conformer. Here, NMR spectra obtained at both atmospheric and high pressures indicate that the population of *cis*-Pro falls well below previous estimates, an effect attributed to the use of short peptides with charged termini in most prior model studies. For the intrinsically disordered protein  $\alpha$ -synuclein, *cis*-Pro populations at all of its five X–Pro bonds are less than 5%, with only modest ionic strength dependence and no detectable effect of the previously demonstrated interaction between the N- and C-terminal halves of the protein. Comparison to small peptides with the same amino-acid sequence indicates that peptides, particularly those with unblocked, oppositely charged amino and carboxyl end groups, strongly overestimate the amount of *cis*-Pro.

Within proteins, the vast majority (>99.5%) of peptide bonds not involving proline exist in the *trans* conformation, in which the dihedral angle ( $\omega$ ) is 180°. The lowly populated *cis* conformer requires 180° rotation about the planar CO(*i*–1)–N(*i*) peptide bond ( $\omega=0^\circ$ ), but such a rotation induces steric clash between the C $^\alpha$ (*i*–1) and C $^\alpha$ (*i*) atoms. This creates a free-energy difference between the *trans* and *cis* conformations of approximately 2–6 kcal mol<sup>–1</sup> in non-Pro peptide bonds, and a high energy barrier to rotation of the partial double bond ( $\approx 20$  kcal mol<sup>–1</sup>) overwhelmingly favors the *trans* state.<sup>[1–3]</sup> However, in peptide bonds between any amino acid (X) and proline (X–Pro), the *trans* and *cis* conformers have a substantially lower energy difference owing to the cyclic nature of the proline side chain. Thus, *cis*-peptidyl-prolyl (*cis*-Pro) conformations in unfolded polypeptide chains are populated to significantly higher levels, with values that range from 5 to 80% in model peptides,<sup>[4–13]</sup> depending on the precise amino-acid composition, with virtually no detectable dependence on temperature.<sup>[11,14]</sup> In folded proteins, local interactions around X–Pro bonds typically induce 100% population of either the *cis* or *trans* conformation.<sup>[15–17]</sup>

*cis*-Pro bonds and their slow isomerization to the *trans* state, approximately 10<sup>–3</sup> to 10<sup>–2</sup> s<sup>–1</sup> at room temperature, depending on the types of adjacent residues,<sup>[12]</sup> can be the rate-limiting step in protein folding,<sup>[2]</sup> as most non-native *cis*-Pro bonds in the unfolded protein require isomerization to the native *trans* conformations for folding to proceed. Indeed, a class of molecular chaperones has evolved to catalyze *cis*–*trans* proline isomerization in nascent polypeptides,<sup>[18]</sup> and in vitro refolding studies have demonstrated that such peptidyl-prolyl isomerases, including the ribosome-localized trigger factor,<sup>[19]</sup> enhance the rate of protein folding.<sup>[20]</sup>

The human proteome contains 6.3% proline residues,<sup>[21]</sup> and intrinsically disordered proteins (IDPs) generally contain primary sequences that are enriched in proline by nearly a factor of two over folded proteins.<sup>[22]</sup> Biologically relevant post-translational modifications occur at numerous Ser/Thr–Pro motifs, and some kinases and phosphatases specifically recognize either the *cis*- or *trans*-Pro conformation.<sup>[23]</sup> Moreover, in chemically denatured proteins used for in vitro folding studies, native *trans*-Pro bonds will isomerize to the *cis* state upon denaturation and equilibration. For proteins with multiple Pro residues, knowledge of the fraction of *cis*-Pro at each X–Pro bond is critical for the resultant analysis of refolding, which typically contains multiple phases. However, the quantification of *cis*-Pro propensity in intact, denatured proteins has remained limited,<sup>[8,14,24]</sup> with most studies instead opting to quantify *cis*-Pro populations in small, model peptides.<sup>[4–7,9–13]</sup>

Despite the often low abundance of *cis*-Pro conformers, NMR spectroscopy is well suited to characterize these states, as *cis*–*trans* Pro isomerization is in the slow exchange regime on the NMR timescale. Therefore, separate resonances for the minor *cis* states are observable. Multidimensional NMR spectroscopy provides a spectroscopic probe at every backbone amide moiety, which thereby enables the accurate, quantitative analysis of *cis*-Pro populations from multiple residues affected by the same Pro, as well as the structural impact of this isomerization. Herein, we employed two- and three-dimensional solution-state NMR spectroscopy to quantify accurately the fractions of *cis*-Pro at 15 different X–Pro bonds in three unfolded proteins, an IDP (i.e.,  $\alpha$ -synuclein) and two pressure-denatured proteins (i.e.,  $\alpha$ -crystallin domain of HSP27 (cHSP27) and ubiquitin V17A/V26A). Comparison of these fractions to those measured for small peptides of identical sequence reveal that peptides tend to overestimate the fraction of *cis*-Pro, in particular if the peptides contain oppositely charged N-terminal amino and C-terminal carboxyl groups. The relatively uniform impact of *cis*-Pro on the chemical shifts of nearby residues will facilitate identification of *cis*-Pro conformers in future NMR spectroscopy studies of IDPs and intrinsically disordered regions (IDRs) of proteins.

[a] T. R. Alderson, Dr. J. H. Lee, Dr. C. Charlier, Dr. J. Ying, Dr. A. Bax  
Laboratory of Chemical Physics, National Institutes of Health  
5 Memorial Drive, Bethesda, MD 20892 (USA)  
E-mail: bax@nih.gov

Supporting Information and the ORCID identification numbers for the authors of this article can be found under <https://doi.org/10.1002/cbic.201700548>.

IDPs typically yield a single set of intense crosspeaks in the two-dimensional (2D)  $^1\text{H}$ ,  $^{15}\text{N}$  HSQC spectrum. The HSQC spectrum of  $\alpha$ -synuclein ( $\alpha\text{S}$ ) exemplifies such behavior, but weak signals from alternate conformers are observable at low contour levels (Figure 1; Figure S1 in the Supporting Information).

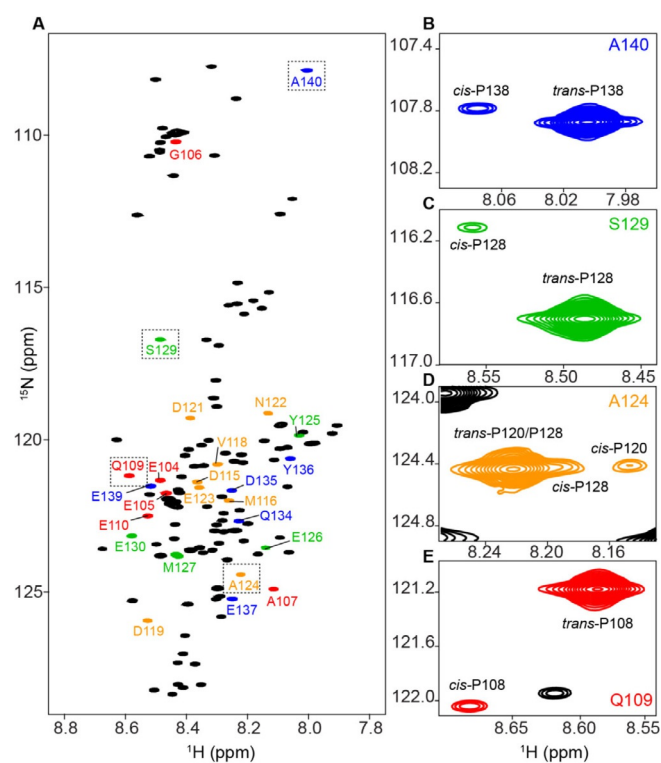


**Figure 1.** Identification of *cis*-Pro bonds in  $\alpha\text{S}$ . A) 2D  $^1\text{H}$ ,  $^{15}\text{N}$  HSQC of 0.9 mM  $^{13}\text{C}$ ,  $^{15}\text{N}$ - $\alpha\text{S}$  at pH 6, 288 K. Resonances impacted by the *cis/trans* state of nearby Pro residues are colored (P108, red; P117, P120, P128, green; P138, blue). B)–E) Zoomed-in regions corresponding to the boxed areas from (A) are shown at a lower contour level. The major *trans* and minor *cis*-Pro peaks are indicated with their assignments. See Figure S1 for the full, low-contour spectrum.

There are five Pro residues in the acidic C-terminal region of  $\alpha\text{S}$ , and the minor signals corresponding to *cis*-Pro bonds cluster near resonances of residues that are close in sequence to Pro. To assign the chemical shifts from the *cis*-Pro conformers in  $\alpha\text{S}$ , triple-resonance NMR spectra were acquired on a 0.9 mM  $[\text{U-}^{13}\text{C}, ^{15}\text{N}]$ -labeled sample. High signal-to-noise ratios in these spectra afforded unambiguous assignment of the residues in the vicinity of all *cis*-Pro conformers (P108, P117, P120, P128, P138), despite the low population of these states (3–4.5%; i.e., 27–40  $\mu\text{M}$  effective sample concentration).

In the *cis*-Pro state, the  $i-1$  residue with respect to Pro shows significant upfield changes in chemical shifts for  $^1\text{H}^{\text{N}}$  ( $\approx \Delta\delta = 0.2-0.4$  ppm) and  $^{15}\text{N}$  ( $\approx \Delta\delta = 2-4$  ppm), with a smaller and usually upfield shift for  $^{13}\text{C}^{\alpha}$  (Figure S2). The small, downfield shift of E137  $^{13}\text{C}^{\alpha}$ , in close proximity to the C terminus, is an exception to this rule. Another diagnostic chemical shift change in the *cis* state is seen for the  $i-2$   $^{13}\text{C}'$  resonance, which exhibits a substantial upfield change ( $\approx \Delta\delta = 0.4-1$  ppm) that is similar in sign and magnitude to the  $^{13}\text{C}'$  chemi-

cal shift change of the isomerizing Pro. Residues in the  $i+1$  and  $i+2$  positions show downfield  $^1\text{H}^{\text{N}}$  chemical shift changes in the *cis* state (up to  $\Delta\delta = 0.2$  ppm) but variable  $^{15}\text{N}$  chemical shift differences. The chemical shift differences typically become vanishingly small for residues in the  $i\pm 4$  positions and beyond.

Using the intensities of the resonances impacted by the *cis* and *trans* states, the *cis*-Pro population was calculated as  $[\textit{cis}]/([\textit{cis}] + [\textit{trans}])$ . In  $\alpha\text{S}$ , the fraction of *cis*-Pro ranged from 3 to 4.5%, which is significantly lower than the values generally reported in the literature (e.g., 10–20%).<sup>[13]</sup> The fraction of *cis*-Pro was highly consistent among the various impacted residues near a given Pro, and the signal-to-noise ratio for each *cis*-Pro-impacted crosspeak was close to approximately 80:1; this indicated the high precision of these measurements.

To compare the *cis*-Pro values in  $\alpha\text{S}$  to values of *cis*-Pro in small peptides of identical sequence, natural abundance NMR spectra were acquired for a set of tetrapeptides (Ac-XXPX-NH<sub>2</sub>) that were N-terminally acetylated and C-terminally amidated. All of the blocked, tetrapeptides, except that corresponding to P120, displayed a significantly higher population of *cis*-Pro than full-length  $\alpha\text{S}$  (Figure 2); this indicated that longer range

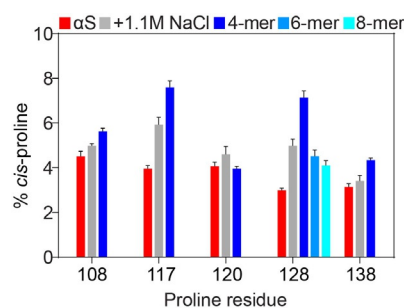


**Figure 2.** Fractions of *cis*-Pro bonds in  $\alpha\text{S}$  and comparison to oligopeptides. All samples were at pH 6, 288 K. The fraction of *cis*-Pro is shown for each Pro residue in  $\alpha\text{S}$  (red), with error bars representing one standard deviation from the mean. Upon the addition of 1160 mM NaCl, the fraction of *cis*-Pro increases (gray); this is indicative of decreased electrostatic repulsion in the acidic C-terminal region of  $\alpha\text{S}$ . Blocked, tetrapeptides (blue), in general, contain elevated levels of *cis*-Pro, whereas hexa- (teal) and octapeptides (cyan) approach the values seen in full-length  $\alpha\text{S}$ .

interactions, presumably steric clashing or repulsive electrostatic interactions of the chains, were unfavorable to the formation of the *cis* state at P108, P117, P128, and P138. The highly negatively charged nature of the carboxy-terminal tail of  $\alpha\text{S}$  (net charge of  $-14$  for the last 40 residues) is expected to enhance the electrostatic contribution. Indeed, at very high ionic strength (1.1 M NaCl), increased *cis* fractions were observed, although the fractions remained below those of the blocked tetrapeptides (Figure 2).

High fractions of *cis*-Pro were previously reported for peptides with an aromatic residue in the  $i-1$  position;<sup>[25]</sup> however, these peptides were mostly studied with unblocked, charged terminal residues. For example, a high *cis* fraction was previously reported for the Phe-Pro-Ala tripeptide.<sup>[7]</sup> However, charge neutralization by N-terminal acetylation and C-terminal amidation reduced the *cis*-Pro fraction by more than one-fifth

(Figure S3). Analogously, the addition of 1.1 M NaCl to the unblocked peptide decreased *cis*-Pro by nearly the same fraction (Figure S3). In the tripeptide Met-Pro-Ser, corresponding to M127-P128-S129 in  $\alpha$ S, we observed even larger reductions in the *cis* fraction upon the addition of blocking groups at the termini or 1.1 M NaCl, which decreased the *cis*-Pro fraction by about a third or a quarter, respectively (Figure S3). Similar results were obtained for the peptide Ala-Pro-Gln, corresponding to A107-P108-Q109 in  $\alpha$ S, which displayed fractional changes in the *cis* content of 43 and 17% upon terminal blockage and the addition of 1.1 M NaCl (Figure S3). Therefore, electrostatic attraction between oppositely charged termini enhances the *cis*-Pro fraction in oligopeptides.

As P128 showed the largest discrepancy between values obtained for full-length  $\alpha$ S and its corresponding blocked tetrapeptide, the impact of longer range interactions on *cis*-Pro was assessed by comparing the fraction of *cis*-Pro at P128 as a function of peptide length. Upon increasing the length of the peptide from four to six to eight residues (Figure 2), a progres-

sive decrease in the fraction of *cis*-Pro was observed. However, even though the blocked octapeptide exhibited a *cis*-Pro fraction that approached that of full-length  $\alpha$ S, the remaining significant difference of 1.5% must have resulted from weak interactions that extended beyond the  $\pm 4$  residue range.

We therefore also evaluated the impact on *cis*-Pro formation in full-length  $\alpha$ S from potential interdomain contacts. Previous NMR spectroscopy measurements indicated that the oppositely charged N- and C-terminal regions of  $\alpha$ S transiently contact each other,<sup>[26,27]</sup> an effect held responsible for the compaction of the radius of hydration of this molecule relative to that of a fully random coil,<sup>[28]</sup> and decreased amyloidogenicity relative to that of sequences that lacked the C-terminal tail.<sup>[29]</sup> Moreover, the N and C termini have been observed to make transient intermolecular contacts.<sup>[30]</sup> Depending on the nature of such contacts, they could either restrict or favor *cis*-Pro formation. However, a construct comprising residues 87–140 of  $\alpha$ S<sup>[31]</sup> showed no detectable differences in the populations of *cis*-Pro between the full-length and truncated proteins (Figure 3); this

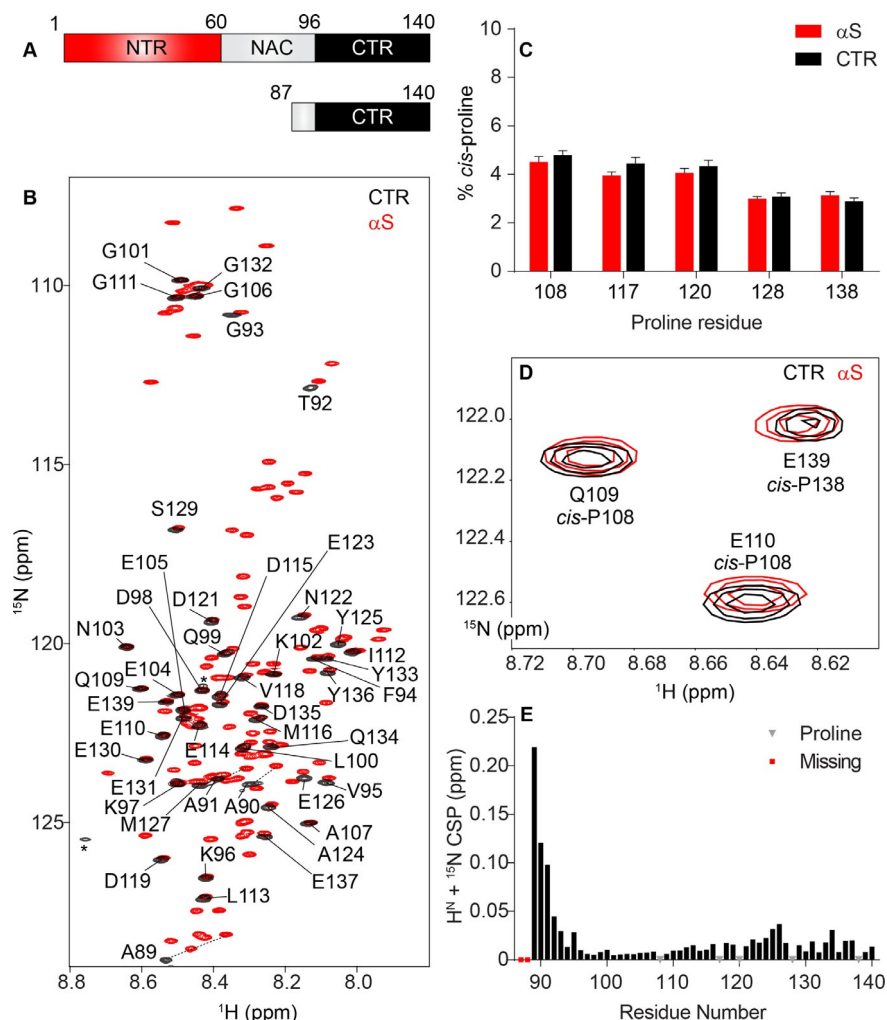


**Figure 3.** The isolated C-terminal region of  $\alpha$ S retains its native *cis*-Pro fractions. A) Depiction of  $\alpha$ S and its three regions: the amphipathic N-terminal region (NTR), the hydrophobic non-amyloid- $\beta$ -containing (NAC) region, and the acidic C-terminal region (CTR). The isolated CTR (bottom) contains an S87C mutation. B) 2D  $^1\text{H}$ ,  $^{15}\text{N}$  HSQC spectra of full-length  $\alpha$ S (red) and the isolated CTR (black). Buffer conditions were as in Figure 1, except that 5 mM 2-mercaptoethanol (BME) was added to the isolated CTR to prevent disulfide formation. The peak indicated with an asterisk arises from an impurity. C) Quantification of the *cis*-Pro fractions in both full-length  $\alpha$ S and its isolated CTR. D) Zoomed-in region from panel B showing resonances affected by *cis*-Pro. E) Combined and weighted  $^1\text{H}$  and  $^{15}\text{N}$  chemical-shift perturbations (CSPs) between full-length  $\alpha$ S and its isolated CTR.

indicated that the N-terminal region did not measurably impact *cis*-Pro propensities in the C-terminal region. Nevertheless, the small chemical shift differences between the full-length protein and this C-terminal 54-residue peptide (Figure 3E) are consistent with the previously noted interactions between the two domains but are too weak to cause a detectable impact on the fraction of *cis*-Pro. To compare the amount of *cis*-Pro in  $\alpha$ S with other unfolded proteins, we used high-pressure NMR spectroscopy, which was previously shown to have no significant effect on the structure and dynamics of  $\alpha$ S.<sup>[32]</sup> To verify that hydrostatic pressure did not impact the *cis*-Pro content in an unfolded protein, we also measured the

fraction of *cis*-Pro in  $\alpha$ S at 250 MPa. Indeed, these values were found to be unchanged with respect to their 0.1 MPa counterparts (Figure S4).

Two proteins were denatured at 250 MPa, and their NMR signals corresponding to residues impacted by *cis*-Pro were assigned. The  $\alpha$ -crystallin domain of HSP27 (cHSP27), a 2  $\times$  10 kDa noncovalent dimer, contains seven Pro residues per subunit that all adopt the *trans* conformation in the native state.<sup>[33]</sup> cHSP27 readily unfolds at high pressures (Figure 4A), and 3D NMR spectra were recorded at 250 MPa to assign the chemical shifts of the pressure-denatured state at pH 7 and 288 K. Previous data indicated that *cis*-Pro populations were in-

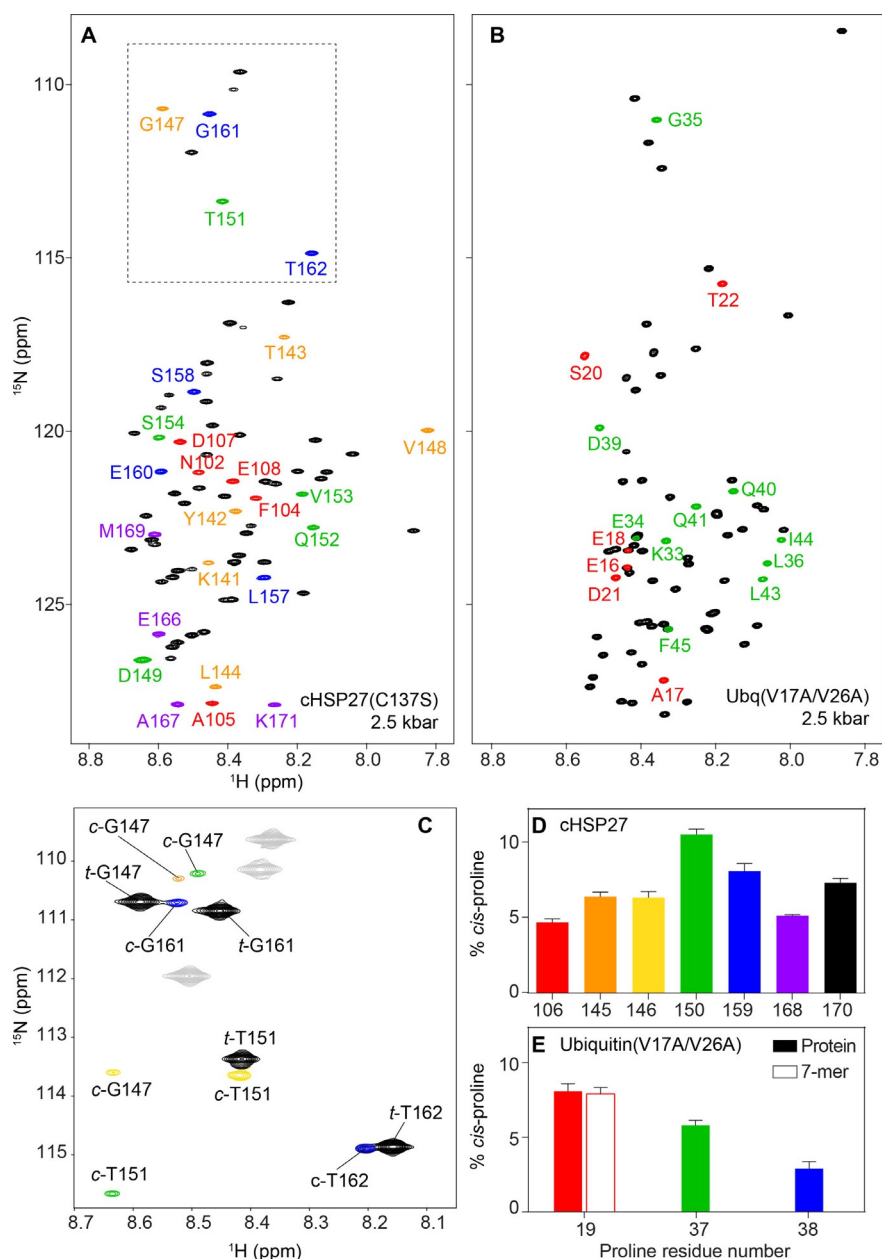


**Figure 4.** Quantification of *cis*-Pro bonds in two pressure-denatured proteins. A) 1.6 mM  $^{13}\text{C}$ ,  $^{15}\text{N}$ -labeled  $\alpha$ -crystallin domain of HSP27 (cHSP27) at 250 MPa in 30 mM sodium phosphate, pH 7, 2 mM ethylenediaminetetraacetic acid (EDTA), 2 mM benzamidine, 288 K. B) 0.75 mM  $^2\text{H}$ ,  $^{13}\text{C}$ ,  $^{15}\text{N}$ -labeled ubiquitin-(V17A/V26A) at 250 MPa in 20 mM potassium phosphate buffer, pH 6.4, 2 mM benzamidine, 288 K. In both (A) and (B), colored resonances have distinguishable assignments for the *trans* and *cis* conformations. C) Boxed region of (A) at a lower contour level; c and t denote *cis* and *trans*, respectively. D), E) Average *cis*-Pro fraction at each Pro residue for the samples in (A) and (B).

dependent of pH for all X–Pro bonds, excluding His–Pro and Tyr–Pro,<sup>[13]</sup> neither of which exist in cHSP27. At least 32 out of 86 <sup>1</sup>H–<sup>15</sup>N correlations in cHSP27 were visibly impacted by *cis*-Pro formation (Figure 4B). Interestingly, cHSP27 contained Pro clustering, with a P145–P146 pair close to P150 and P168 near P170. As a result, nearby residues were affected by *cis*–*trans* isomerization from multiple X–Pro bonds. For example, four signals were observed for G147: all *trans*, *cis*-P145, *cis*-P146, and *cis*-P150 (Figure 4C), and sequential assignments provided unambiguous identification of each X–Pro bond of interest. As compared to  $\alpha$ S, the amount of *cis*-Pro in pressure-denatured cHSP27 varied widely, from 5 to 10% across the seven X–Pro bonds (Figure 4D).

Ubiquitin contains three Pro residues, but the wild-type protein does not easily unfold at high pressure. Therefore, a cavity-containing double mutant (V17A/V26A)<sup>[33]</sup> was prepared to facilitate pressure-induced unfolding. These mutations lowered the midpoint of pressure denaturation from > 500 MPa to approximately 140 MPa, and this enabled the acquisition of a set of 3D NMR spectra to assign the minor signals corresponding to *cis*-Pro (Figure 4B). The *cis*-Pro fraction varied by a factor of three across the Pro residues, from as low as 2.5% at P38, which follows P37, to 8% at P19 (Figure 4E). A heptapeptide of the same amino-acid composition centered around P19 exhibited the same fraction of *cis*-Pro as full-length, pressure-unfolded ubiquitin (Figure 4E). The P37–P38 bond in ubiquitin (V17A/V26A) displayed the lowest *cis*-Pro value (2.5%) across all 15 X–Pro bonds. However, the chemically similar P145–P146 bond in cHSP27 contained approximately 6% *cis*-Pro, which thus highlighted the importance of residues remote from the Pro–Pro bond.

Our results indicate that the populations of *cis*-Pro conformers in unfolded proteins are considerably lower than those in the corresponding short peptides, which were previously used to estimate these fractions. The presence of *cis*-Pro is often considered a hurdle in protein folding, and with multiple Pro residues per chain, the fraction of all-*trans* X–Pro chains can be strongly impacted by even a modest change in the *cis*-Pro ratios. We attribute the lower *cis*-Pro fractions in the longer polypeptides to increased steric clashing between the segments of the chain preceding and following the *cis* peptide bond, which effectively reverses the chain direction and reduces the conformational space available to the two segments. Electrostatic repulsion between these segments, as applies in  $\alpha$ S, can enhance this effect. The utility of high-pressure NMR spectroscopy to quantify accurately *cis*-Pro populations in proteins is key to on-going studies of protein folding by pressure-jump NMR spectroscopy,<sup>[33–35]</sup> and the reported *cis/trans* chemical shift differences serve as convenient guides for identifying *cis*-Pro-related resonances in NMR-based studies of IDPs and denatured proteins.

Antibody data implicated elevated *cis*-Pro levels in toxic fibril formation of the intrinsically disordered Tau protein, associated with traumatic brain injury,<sup>[36]</sup> but NMR spectroscopy data refuted this conclusion.<sup>[14]</sup> In the context of  $\alpha$ S and its formation of amyloid fibrils, mutation of its Pro residues to Ala accelerates fibril formation.<sup>[37]</sup> Considering that the C-terminal

region does not become embedded in the fibril core,<sup>[38]</sup> this points to a possible inhibitory role of *cis*-Pro in fibril elongation, for which a low *cis* fraction would suffice for such a role. The NMR spectra of  $\alpha$ S obtained in living bacterial and mammalian cells<sup>[39–41]</sup> indicate that  $\alpha$ S retains its predominantly *trans*-Pro conformation, which implies that in vivo interactions do not drastically alter the inherent *cis*-Pro propensities of  $\alpha$ S.

## Experimental Section

Isotopically labeled proteins were expressed in *E. coli* and were purified as described in the Supporting Information. All NMR spectra were acquired with Bruker Avance III spectrometers (700 and 800 MHz) equipped with cryogenically cooled probes. The amino-acid sequences of the oligopeptides and proteins used in this study are listed in Tables S1 and S2, respectively. Additional experimental details can be found in the Supporting Information.

## Acknowledgements

We thank James L. Baber, Yang Shen, and Daniel Garrett for technical support; Julien Roche, Robert Best, and Dennis A. Torchia for insightful discussions; Zhiping Jiang and Jennifer C. Lee (NHLBI) for the plasmid coding for the C-terminal region of  $\alpha$ S; Justin Benesch, Andrew Baldwin, and Heidi Gastall (University of Oxford) for the plasmid encoding cHSP27; John Lloyd at the NIDDK Mass Spectrometry Core Facility; and Galina Abdoulaeva (CBER/FDA) for peptide synthesis. This work was supported by the Intramural Research Program of the National Institute of Diabetes and Digestive and Kidney Diseases and by the Intramural Antiviral Target Program of the Office of the Director, NIH.

## Conflict of Interest

The authors declare no conflict of interest.

**Keywords:** alpha-synuclein • cis-proline • high pressure • isomerization • NMR spectroscopy • protein folding

- [1] M. S. Weiss, A. Jabs, R. Hilgenfeld, *Nat. Struct. Mol. Biol.* **1998**, *5*, 676.
- [2] W. J. Wedemeyer, E. Welker, H. A. Scheraga, *Biochemistry* **2002**, *41*, 14637–14644.
- [3] C. Dugave, L. Demange, *Chem. Rev.* **2003**, *103*, 2475–2532.
- [4] C. M. Deber, D. A. Torchia, S. C. Wong, E. R. Blout, *Proc. Natl. Acad. Sci. USA* **1972**, *69*, 1825–1829.
- [5] D. A. Torchia, *Biochemistry* **1972**, *11*, 1462–1468.
- [6] C. Grathwohl, K. Wuthrich, *Biopolymers* **1976**, *15*, 2043–2057.
- [7] C. Grathwohl, K. Wuthrich, *Biopolymers* **1981**, *20*, 2623–2633.
- [8] S. K. Sarkar, P. E. Young, C. E. Sullivan, D. A. Torchia, *Proc. Natl. Acad. Sci. USA* **1984**, *81*, 4800–4803.
- [9] H. J. Dyson, M. Rance, R. A. Houghten, R. A. Lerner, P. E. Wright, *J. Mol. Biol.* **1988**, *201*, 161–200.
- [10] J. Yao, V. A. Feher, B. F. Espejo, M. T. Reymond, P. E. Wright, H. J. Dyson, *J. Mol. Biol.* **1994**, *243*, 736–753.
- [11] D. P. Raleigh, P. A. Evans, M. Pitkeathly, C. M. Dobson, *J. Mol. Biol.* **1992**, *228*, 338–342.
- [12] U. Reimer, G. Scherer, M. Drewello, S. Kruber, M. Schutkowski, G. Fischer, *J. Mol. Biol.* **1998**, *279*, 449–460.
- [13] S. Osváth, M. Gruebele, *Biophys. J.* **2003**, *85*, 1215–1222.

- [14] P. Ahuja, F.-X. Cantrelle, I. Huvent, X. Hanouille, J. Lopez, C. Smet, J.-M. Wieruszkeski, I. Landrieu, G. Lippens, *J. Mol. Biol.* **2016**, *428*, 79–91.
- [15] A. P. Capaldi, S. J. Ferguson, S. E. Radford, *J. Mol. Biol.* **1999**, *286*, 1621–1632.
- [16] P. Sarkar, C. Reichman, T. Saleh, R. B. Birge, C. G. Kalodimos, *Mol. Cell* **2007**, *25*, 413–426.
- [17] K. P. Lu, G. Finn, T. H. Lee, L. K. Nicholson, *Nat. Chem. Biol.* **2007**, *3*, 619–629.
- [18] F. X. Schmid, *Annu. Rev. Biophys. Biomol. Struct.* **1993**, *22*, 123–143.
- [19] T. Hesterkamp, S. Hauser, H. Lütcke, B. Bukau, *Proc. Natl. Acad. Sci. USA* **1996**, *93*, 4437–4441.
- [20] K. Lang, F. X. Schmid, G. Fischer, *Nature* **1987**, *329*, 268–270.
- [21] A. A. Morgan, E. Rubenstein, D. Hosack, J. Yang, W. Gao, *PLoS One* **2013**, *8*, e53785.
- [22] F.-X. Theillet, L. Kalmar, P. Tompa, K.-H. Han, P. Selenko, A. K. Dunker, G. W. Daughdrill, V. N. Uversky, *Intrinsically Disord. Proteins* **2013**, *1*, e24360.
- [23] J. W. Werner-Allen, C.-J. Lee, P. Liu, N. I. Nicely, S. Wang, A. L. Greenleaf, P. Zhou, *J. Biol. Chem.* **2011**, *286*, 5717–5726.
- [24] T. R. Alderson, J. L. P. Benesch, A. J. Baldwin, *Cell Stress Chaperones* **2017**, *22*, 639–651.
- [25] K. M. Thomas, D. Naduthambi, N. J. Zondlo, *J. Am. Chem. Soc.* **2006**, *128*, 2216–2217.
- [26] C. W. Bertoncini, Y.-S. Jung, C. O. Fernandez, W. Hoyer, C. Griesinger, T. M. Jovin, M. Zweckstetter, *Proc. Natl. Acad. Sci. USA* **2005**, *102*, 1430–1435.
- [27] C. C. Rospigliosi, S. McClendon, A. W. Schmid, T. F. Ramlall, P. Barré, H. A. Lashuel, D. Eliezer, *J. Mol. Biol.* **2009**, *388*, 1022–1032.
- [28] V. N. Uversky, J. Li, A. L. Fink, *J. Biol. Chem.* **2001**, *276*, 10737–10744.
- [29] W. Hoyer, D. Cherny, V. Subramaniam, T. M. Jovin, *Biochemistry* **2004**, *43*, 16233–16242.
- [30] Z. Jiang, F. Heinrich, R. P. McGlinchey, J. M. Gruschus, J. C. Lee, *J. Phys. Chem. Lett.* **2017**, *8*, 29–34.
- [31] J. Roche, J. Ying, A. S. Maltsev, A. Bax, *ChemBioChem* **2013**, *14*, 1754–1761.
- [32] G. K. Hochberg, H. Ecroyd, C. Liu, D. Cox, D. Cascio, M. R. Sawaya, M. P. Collier, J. Stroud, J. A. Carver, A. J. Baldwin, C. V. Robinson, D. S. Eisenberg, J. L. Benesch, A. Laganowsky, *Proc. Natl. Acad. Sci. USA* **2014**, *111*, E1562–E1570.
- [33] T. R. Alderson, C. Charlier, D. A. Torchia, P. Anfinrud, A. Bax, *J. Am. Chem. Soc.* **2017**, *139*, 11036–11039.
- [34] W. Kremer, M. Arnold, C. E. Munte, R. Hartl, M. B. Erlach, J. Koehler, A. Meier, H. R. Kalbitzer, *J. Am. Chem. Soc.* **2011**, *133*, 13646–13651.
- [35] J. Roche, M. Dellarole, J. A. Caro, D. R. Norberto, A. E. Garcia, B. Garcia-Moreno, C. Roumestand, C. A. Royer, *J. Am. Chem. Soc.* **2013**, *135*, 14610–14618.
- [36] A. Kondo, K. Shahpasand, R. Mannix, J. Qiu, J. Moncaster, C.-H. Chen, Y. Yao, Y.-M. Lin, J. A. Driver, Y. Sun, S. Wie, M.-L. Luo, O. Albayram, P. Huang, A. Rotenberg, A. Ryo, L. E. Goldstein, A. Pascual-Leone, A. C. McKee, W. Meehan, X. Z. Zhou, K. P. Lu, *Nature* **2015**, *523*, 431–436.
- [37] J. Meuvius, M. Gerard, L. Desender, V. Baekelandt, Y. Engelborghs, *Biochemistry* **2010**, *49*, 9345–9352.
- [38] M. D. Tuttle, G. Comellas, A. J. Nieuwkoop, D. J. Covell, D. A. Berthold, K. D. Kloepper, J. M. Courtney, J. K. Kim, A. M. Barclay, A. Kendall, W. Wan, G. Stubbs, C. D. Schwieters, V. M. Lee, J. M. George, C. M. Rienstra, *Nat. Struct. Mol. Biol.* **2016**, *23*, 409–415.
- [39] A. Binolfi, F. X. Theillet, P. Selenko, *Biochem. Soc. Trans.* **2012**, *40*, 950–954.
- [40] A. Binolfi, A. Limatola, S. Verzini, J. Kosten, F. X. Theillet, H. M. Rose, B. Bekei, M. Stuiiver, M. van Rossum, P. Selenko, *Nat. Commun.* **2016**, *7*, 10251.
- [41] F. X. Theillet, A. Binolfi, B. Bekei, A. Martorana, H. M. Rose, M. Stuiiver, S. Verzini, D. Lorenz, M. van Rossum, D. Goldfarb, P. Selenko, *Nature* **2016**, *530*, 45–50.

---

Manuscript received: October 10, 2017

Accepted manuscript online: October 24, 2017

Version of record online: November 16, 2017